Proceedings of the 18th World Congress
The International Federation of Automatic Control
Milano (Italy) August 28 - September 2, 2011

Model Predictive Control for Automotive Engine Torque considering Internal Exhaust Gas Recirculation

T. Jimbo * **Y. Hayakawa** **

* *Toyota Central R&D Labs.,inc., Nagakute, Aichi 480-1192, Japan (e-mail: t-jmb@mosk.tytlabs.co.jp).*
** *Department of Mechanical Science and Engineering, Nagoya University, Nagoya, Aichi 464-8603, Japan (e-mail: hayakawa@nuem.nagoya-u.ac.jp)*

Abstract: The present paper introduces a control oriented model based on air and burned gas flows for automotive engines with variable valves. Moreover, a predictive controller is proposed by using the obtained model. For the engines with variable valves, the intake valve lift enables the quick torque response; on the other hand, the large valves' overlap may cause a misfiring of combustion because of the increase of the burned gas into a cylinder. Therefore, the control purpose is to track not only the torque reference but also the pressure reference of surge tank in consideration for the constraint of IEGR ratio. In the proposed control design, the mass flows through the throttle and the intake valves are designed as virtual control inputs. Effectiveness of the proposed controller is demonstrated by the SICE benchmark simulator.

Keywords: spark ignition engine, internal exhaust gas recirculation, modeling, predictive control, constraints, quadratic programming, No offset, physical-model-based control

1. INTRODUCTION

An engine torque is demanded from other systems such as vehicle dynamics control and transmission control. Moreover, engine systems are required to reduce the fuel consumption and exhaust emissions. In order to address those issues, the systems have become increasingly complex. For example, the systems have multiple inputs such as the intake valve lift, the intake and exhaust valve timings in addition to the throttle valve.

Recently, there have been a lot of attention to torque control for automotive engines as in Jankovic et al. (1998), Ingram et al. (2003), Huang et al. (2008), and Gruenbacher et al. (2008). For the engines with variable valves, the intake valve lift enables the quick torque response; on the other hand, the large valves' overlap may cause a misfiring of combustion because of the increase of the burned gas into a cylinder. Therefore, a controller must be also required to consider IEGR (Internal Exhaust Gas Recirculation).

Model predictive control (MPC) has been actively researched and is one of the most suitable method to deal with constraints of control inputs and states (Mayne et al. (2000) and Maciejowski (2002)). Recently, MPC has been applied to automotive engines (Langthaler and del Re (2008), Muske et al. (2008), and del Re et al. (2010)).

The present paper considers the torque control for spark ignition engines with variable valves in Figure 1. A control oriented model is derived based on air and burned gas flows. Moreover, a predictive controller is proposed by using the obtained model. The control purpose is to track not only the torque reference but also the pressure reference of surge tank in consideration for the constraint of IEGR ratio. The control inputs are the throttle angle and the intake valve lift. In the proposed control design, the mass flows through the throttle and the intake valves are regarded as virtual control inputs.

Section 2 introduces a control oriented model. As in Jimbo and Hayakawa (2011a), for a system with both time-dependent and crank angle-dependent dynamics, a discrete-crank angle modeling is proposed for the engine with variable valves. State equation is derived from the discrete-crank angle model. In Section 3, a predictive controller is proposed by using the obtained model. Constrains of bounds of inputs and IEGR ratio are transformed into ones of the flows (the virtual control inputs). The optimal mass flows are designed by a predictive controller considering the transformed constraints. An offset-free control to reference signals is realized by using a observer. Section 4 demonstrates the effectiveness of the proposed controller by numerical simulations. The conclusion is presented in Section 5.

NOTATIONS

P_o, P_a, P_e	pressures of outer air, the surge tank (called intake pressure), and the exhaust confluence point
T_o, T_a, T_e	temperatures of outer air, the surge tank, and the exhaust confluence point
M_t, M_{iv}, M_{back}	masses through the throttle, the intake valve, and mass of the backflow

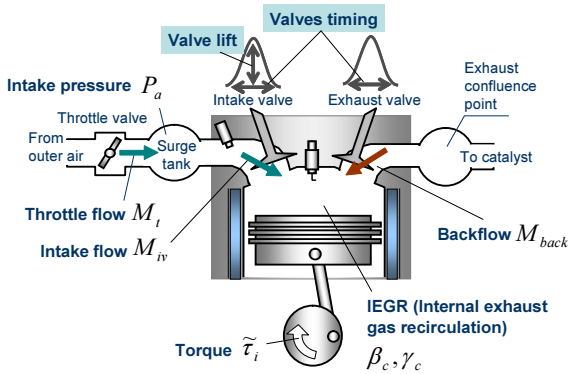

Fig. 1. Controlled plant

$\zeta_1, \zeta_2, \zeta_3$	time-shifted variables of M_{iv}, i.e., $\zeta_1(k-1)=\zeta_2(k)=\zeta_3(k+1)=M_{iv}(k)$
η	prime mass which depends on the intake valve lift
Ψ	nonlinear flow function
A_t	effective opening areas of the throttle
I_{AOL}	angularly-integrated effective opening area of the overlap and depends on θ_{OL} and u_{VL}
u_t, u_{VL}	throttle angle and the intake valve lift
θ_{OL}	overlap period which intake and the exhaust valves open simultaneously
$\tilde{\tau}_i$	filtered indicated torque
ω	engine speed
γ_c, β_c	IEGR (Internal Exhaust Gas Recirculation) ratios
M_{ivo}	mass in a cylinder at intake valve open
k, h_d, h_w	sampling point, sampling interval, and sampling time

2. AIR/BURNED GAS FLOW-BASED CONTROL ORIENTED MODELING

For the torque control problem with constraints of the bounds of control inputs and the IEGR ratio, in this section, a control design method based on models of air and burned gas flows is proposed.

A number of previous studies have examined the modeling of internal combustion engines shown in Figure 1(Taylor (1985)). The gas flow such as the throttle, the intake, and the exhaust valves is described in Liepmann and Roshko (1960), Heywood (1988). And a backflow model of the burned gas into the cylinder is studied in Leroy et al. (2008).

As in Jimbo and Hayakawa (2011b), the control oriented discrete-crank angle models (1) through (6) are derived from the fundamental equations of internal combustion engines. Here, as in Jimbo and Hayakawa (2011a), the sampling points $k, k+1, \cdots$ are chosen as instants the strokes end. As a result, the sampling interval is $h_d = 4\pi/N_{cyl}$[rad], the sampling time $h_w = h_d/\omega[s]$, where N_{cyl} is number of cylinders. In the case of six cylinders, when the exhaust valve of a cylinder closes at sampling point $k-2$, the intake valve of the cylinder closes at k and the combustion stroke ends at $k+2$.

$$M_t(k) = h_w A_t(u_t(k))\Psi(P_a(k)) \tag{1}$$

$$M_{iv}(k) = k_{m_{iv}}\eta(k-2) + k_4(P_a(k-2) - P_e) - k_5 M^{lin}_{back}(k-2) \tag{2}$$

$$M^{lin}_{back}(k) = \begin{cases} I_{AOL}(k)a_3(P_e - P_a(k)), & \dfrac{P_a(k)}{P_e} \geq 2r^{lin}_{chk} - 1 \\ I_{AOL}(k)c_3 P_e & otherwise \end{cases} \tag{3}$$

$$\eta(k) = k_1(u_{VL}(k), \omega)P_a(k) \tag{4}$$

$$P_a(k+1) = P_a(k) + k_8(M_t(k) - M_{iv}(k)) \tag{5}$$

$$\tilde{\tau}_i(k+1) = (1-k_9)\tilde{\tau}_i(k) + k_9\{k_6(P_a(k) - P_e) + k_\tau k_7 M_{iv}(k-1)\} \tag{6}$$

where γ^{lin}_{chk}, k_4, k_5, k_6, k_7, and k_8 are constants, $k_{m_{iv}}$ and k_τ are adjustable parameters. h_w, a_3, c_3, and k_9 are parameters which depend on ω. Note that η is derived from quasi-steady approximation of the cylinder pressure dynamics during the intake stroke, I_{AOL} is assumed to be a constant during the prediction horizon defined in Subsection 3.4.

The IEGR ratios, γ_c and β_c, are defined as

$$\beta_c(k) = \frac{\gamma_c(k)}{1+\gamma_c(k)}, \quad \gamma_c(k) = \frac{M_{ivo} + M^{lin}_{back}(k-2)}{M_{iv}(k)}. \tag{7}$$

From (1) through (6), the discrete-time state space model is given by

$$\begin{aligned} x(k+1) &= A_x x(k) + B_x v(k) + K_x P_e \\ y(k) &= C_x x(k) \end{aligned} \tag{8}$$

where $x(k) = [P_a(k), \zeta_1(k), \zeta_2(k), \zeta_3(k), \tilde{\tau}_i(k)]^T$ is the state, $v(k) = [M_t(k), \eta(k)]^T$ is the virtual input, $y(k) = [P_a(k), \tilde{\tau}_i(k)]^T$ is the output, the term $K_x P_e$ is the known disturbance. Note that $\tilde{\tau}_i$ is the filtered variable of the indicated torque which is assumed to be estimated or to be measured. And the exhaust pressure P_e and temperature T_e are assumed to be estimated.

3. CONTROLLER DESIGN

3.1 Steady State

Given the pair of the throttle angle u_t and the intake valve lift u_{VL} or the pair of the intake pressure P_a and the indicated torque τ_i, the steady states are uniquely decided by (8). Here, the latter pair is used. The left and right graphs of Figures 2 show IEGR ratio β_c at the steady states in the cases of valves' overlap $\theta_{OL} = 40$ [degCA] and $\theta_{OL} = 60$ [degCA], respectively, under the condition: engine speed $\omega = 2000$ [rpm], pressures of outer air and exhaust confluence point $P_o = P_e = 101.3$ [kPa], temperature of outer air $T_o = 25$ [degC], temperature of exhaust confluence point $T_e = 400$ [degC], $k_{m_{iv}} = 0.3$, and $k_\tau = 0.95$.

The following is shown from Figures 2.

- In the case of constant intake valve lift, in general, when the intake pressure is low (high), the torque is low (high) and the backflow is high (low). On the other hand, when the intake valve lift is variable, it happens that the intake pressure is high and the torque is low simultaneously.

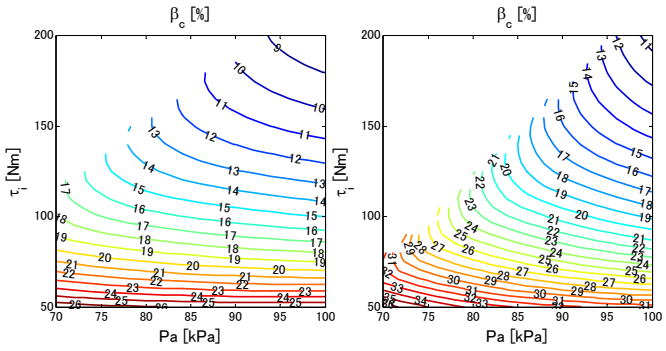

Fig. 2. Steady state β_c (ω=2000[rpm], θ_{OL}=40[deg](left graph) and θ_{OL}=60[deg](right graph))

- It is impossible that low intake pressure causes high torque in the region of the upper left of each graph.
- IEGR ratio β_c is high at low intake pressure. That means the the increase of the mass of the backflow.
- It is found that IEGR ratio β_c is more sensitive to intake pressure P_a in the case of large overlap than the case of small overlap.

Therefore, taking care of the constraint of IEGR ratio is very important in the case of large overlap.

3.2 Constraints

The following constraints are considered from the practical viewpoint:

(a) bounds of input levels
$u_t^{\min} \le u_t \le u_t^{\max}$, $u_{VL}^{\min} \le u_{VL} \le u_{VL}^{\max}$.
(b) bounds of input speeds
$\delta u_t^{\min} \le \delta u_t \le \delta u_t^{\max}$, $\delta u_{VL}^{\min} \le \delta u_{VL} \le \delta u_{VL}^{\max}$.
(c) upper bound of IEGR ratio
$\beta_c \le \beta_c^{\max}$, where $\beta_c^{\max}$ is threshold of misfiring. Note that, considering the prediction error of the IEGR ratio, $\beta_c^{\max}$ is replaced by the virtual upper bound $\tilde{\beta}_c^{\max}$ such that $\tilde{\beta}_c^{\max} < \beta_c^{\max}$.

In the present paper, control design based on flow v is proposed. Therefore, the constraints with respect to u_t and u_{VL} are transformed into mixed constraints of $v(k)$ and $x(k)$.

Constraint **(a)** is transformed into the mixed constraint. For the throttle valve, the following inequality is obtained from (1):

$$M_t^{\min} \le M_t(k) \le M_t^{\max}(k) \tag{9}$$

where $M_t^{\min}$ and $M_t^{\max}$ respectively corresponds to $u_t^{\min}$ and $u_t^{\max}$ in (1). It is assumed that $M_t^{\min} = 0 (u_t^{\min} = 0)$. Here, only for the constraints concerning M_t, the nonlinear flow function Ψ is approximated by a linear one Ψ_{lin}. For the intake valve lift, the following is obtained from (4):

$$\eta^{\min}(k) \le \eta(k) \le \eta^{\max}(k) \tag{10}$$

where $\eta^{\min}$ and $\eta^{\max}$ respectively corresponds to $u_{VL}^{\min}$ and $u_{VL}^{\max}$ in (4).

In a similar fashion, considering $\delta M_t = (\frac{\partial A_t}{\partial u_t}\delta u_t) h_w \Psi_{lin}$ and $\delta\eta = (\frac{\partial k_1}{\partial u_{VL}}\delta u_{VL}) P_a$, constraint **(b)** is transformed into the mixed constraint as below:

$$\delta M_t^{\min}(P_a(k)) \le \delta M_t(k) \le \delta M_t^{\max}(P_a(k)) \tag{11}$$
$$\delta\eta^{\min}(P_a(k)) \le \delta\eta(k) \le \delta\eta^{\max}(P_a(k)) \tag{12}$$

Constraint **(c)** of β_c is transformed into that of γ_c and directly expressed from (7) by the following form of the mixed constraint:

$$M_{ivo} + M_{back}^{lin}(k) \le \tilde{\gamma}_c^{max} M_{iv}(k+2). \tag{13}$$

where $\tilde{\gamma}_c^{\max} = \frac{\tilde{\beta}_c^{\max}}{1-\tilde{\beta}_c^{\max}}$.

As a result, considering (3) and (2), constraints (9) and (10) through (13) are combined to get the following form:

$$C_1^C x(k) + D_2^C v(k) + D_1^C \delta v(k) \le E_1^C p_x \tag{14}$$

where $p_x = [P_e, P_o, M_{ivo}]^T$. C_1^C and E_1^C involve I_{AOL}, which is assumed to be a constant during the prediction horizon defined in Subsection 3.4 as well as (8). Note that the after-mentioned problem (19) is more feasible by replacing $P_a(k)$ by $P_a(k+1)$ in (14) because $P_a(0)$ is the present value.

3.3 Delta input formation

A designed virtual input (mass) $v(k) = [M_t(k), \eta(k)]^T$ is inverted to the actual input $u(k) = [u_t(k), u_{VL}(k)]^T$. But, the actual mass corresponding to $v(k)$ is not necessarily equal to $v(k)$. Therefore, for (8), the following "delta input formulation" equivalent to the approach of input disturbance model is used:

$$v(k) = v(k-1) + \delta v(k). \tag{15}$$

For (8) and (15), the expanded state space model with the new states $v(k-1)$ is given by

$$\begin{aligned} \xi(k+1) &= A\xi(k) + B\delta v(k) + Kp_x \\ y(k) &= C\xi(k) \end{aligned} \tag{16}$$

and for (14) and (15), the mixed constraints are given by

$$C^C \xi(k) + D^C \delta v(k) \le E^C p_x \tag{17}$$

where $\xi(k) = [x(k)^T, v(k-1)^T]^T$, $A \in R^{n\times n}$, $B \in R^{n\times m}$, $K \in R^{n\times n_d}$, $C \in R^{p\times n}$, $C^C \in R^{n_c\times n}$, $D^C \in R^{n_c\times m}$, $E^C \in R^{n_c\times n_d}$, $n = 7$, $m = 2$, $p = 2$, and $n_d = 3$. n_c depends on the number of considered constraints.

3.4 Predictive Controller

An IEGR ratio β_c^* and a filtered indicated torque $\tilde{\tau}_i^*$ are given as reference signals. From the result of the steady state analysis in Subsection 3.1, in the proposed predictive controller, β_c^* is replaced by the intake pressure P_a^*. Let $y(k)$ track reference signal $r(k)$, where $r(k) = [P_a^*(k), \tilde{\tau}_i^*(k)]^T$. Namely, the proposed controller designs the optimal $\delta v(k)$ based on the following objective function:

$$\min_{\delta v(t),\cdots,\delta v(t+N_u-1)} \left\{ \sum_{k=N_w}^{N_p} e(t+k)^T Q e(t+k) + \sum_{k=1}^{N_u} \delta v(t+k-1)^T R \delta v(t+k-1) \right\} \tag{18}$$

subject to (16) and (17), where t is current time, $e(t+k) \triangleq y(t+k) - r(t+k)$, prediction horizon is N_w to

N_p, control horizon is the same as N_p, $Q \in R^{p\times p}$ is a symmetric positive-semidefinite matrix, and $R \in R^{m\times m}$ is a symmetric positive-definite matrix. Note that, given $\tilde{\tau}_i^*$ and β_c^*, steady state P_a^* is calculated as in section 3.1.

Furthermore, assuming that the matrices in (16) and (17) are constants during the prediction horizon, the above tracking problem (18) is transformed into the following quadratic form:

$$\min_U \frac{1}{2}U^T HU + p(t)^T FU \ s.t.\ GU \le W + Ep(t) \quad (19)$$

where $U = [\delta v(t)^T, \cdots, \delta v(t+N_p-1)^T]^T \in R^{mN_p}$, $p(t) = [\xi(t)^T, p_x(t)^T, r(t+1), \cdots, r(t+N_p)]^T \in R^{n+n_d+pN_p}$, $W = 0$.

Let $U^*(p(t))$ be an optimal solution of (19), the optimal variation $\delta v(t)$ at time t consists simply of the first two components of $U^*(p(t))$. The optimal masses $v(t) = [M_t(t), \eta(t)]^T$ are derived from (15), where initial values $v(0)$ are calculated from (1), (3), and (2) by using the measurable values ω, m_t, and P_a. By using the optimal masses $v(t)$, the optimal $u_t(t)$ and $u_{VL}(t)$ are obtained from (1) and (4), respectively.

Figure 3 shows the block diagram of the proposed controller. Here, $\hat{g}^{-1}(\cdot)$ and $g(\cdot)$ indicate the inverse transformation of (1) and (4) and the actual flow, respectively. And **H** and **S** are the zero-order holder and the sampler per 120 deg crank angle, respectively.

In the present paper, the matrices A, B, K, C, C^C, D^C, and E^C in (16) and (17) are assumed to be constants during the prediction horizon. If the matrices are constants all the time, the optimization problem (19) can be preliminarily solved by the multiparametric programming (Bemporad et al. (2002)) to reduce the computational cost in the implementation because the matrices H, F, G, and E in (19) are constants. However, because the matrices A, B, K, C, C^C, D^C, and E^C depend on the engine state (especially, u_{VL} and θ_{OL}), the optimization problem (19) is solved to get the optimal sequence $U^*(p(t))$ by using active set methods at each time step t. Note that, if u_t and u_{VL} are directly designed, the predictive control problem (18) is treated as nonlinear programming to make it more difficult to solve the optimal sequence.

3.5 Observer

To realize an offset-free control to reference signals, i.e., $y(t) \to r(t)$ for $t \to \infty$, the predictive controller uses the estimate value $\hat{v}$ by minimum order observer instead of v of (15) as the present state. That means any plant/model mismatch is lumped into $\hat{v}(\neq v)$, the input disturbance is estimated to realize an offset-free control (Maeder et al. (2009)).

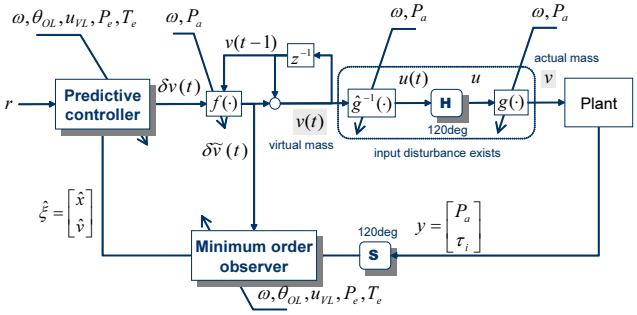

Fig. 3. Block diagram of the proposed controller

Calculating $v(t)$ of (15) using output $\delta v(t)$ of the predictive controller, $v(t)$ may exceed bounds: $v(t) < v^{\min}(P_a(t))$ or $v(t) > v^{\max}(P_a(t))$. Therefore, the following countermeasure is taken:

$$\begin{aligned}\delta\tilde{v}(t) &= f(\delta v(t), v(t-1), v^{\min}(t), v^{\max}(t)) \\ &= \begin{cases} v^{\min}(t) - v(t-1), & v(t) < v^{\min}(t) \\ v^{\max}(t) - v(t-1), & v(t) > v^{\max}(t) \\ \delta v(t), & otherwise \end{cases}\end{aligned} \quad (20)$$

where $v^{\min} = [M_t^{\min}, \eta^{\min}]^T$ and $v^{\max} = [M_t^{\max}, \eta^{\max}]^T$.

4. NUMERICAL SIMULATIONS

Effectiveness of the above proposed controller is demonstrated by the benchmark simulator, which has been provided in SIMULINK® by the SICE Research Committee on Advanced Control of Engines (Ohata et al. (2008)).

The parameters are set in the benchmark simulator and the proposed controller as shown in Table 1. Concerning the other control inputs, the fuel injection is controlled to regulate air-fuel ratio α to be stoichiometric, and spark timing is set to the optimal one from the view point of fuel consumption. And the torque reference $\tilde{\tau}_i^*(t)$ is a stepwise function with $\tilde{\tau}_i^*(t) \in [100, 140]$ [Nm], IEGR reference $\beta_c^*(t)$ is a constant at $\beta_c^* = 20$ [%], The upper bound of IEGR ratio $\beta_c^{\max}(t)$ and the virtual upper bound $\tilde{\beta}_c^{\max}(t)$ are constants at $\beta_c^{\max} = 24$ [%] and $\tilde{\beta}_c^{\max} = 22$ [%], respectively.

In Figures 4 through 9, "ref" and "sim" denote the corresponding reference and the actual value in the benchmark simulator, respectively. For IEGR ratio β_c, "upper", "upper(mpc)", and "mpc" denote the upper bound $\beta_c^{\max}$, the virtual upper bound $\tilde{\beta}_c^{\max}$, and the predicted value $\beta_c(t+2)$, respectively. The predicted ratio $\beta_c(t+2)$ is derived from (3), (2), (7), (15) and (20) as follows:

$$\begin{aligned}\beta_c(t+2) &= \frac{\gamma_c(t+2)}{1+\gamma_c(t+2)} \\ \gamma_c(t+2) &= \frac{M_{ivo} + M_{back}^{lin}(t)}{k_{m_{iv}}\eta(t) + k_4(P_a(t) - P_e) - k_5 M_{back}^{lin}(t)} \\ \eta(t) &= \hat{\eta}(t-1) + \delta\tilde{\eta}(t)\end{aligned} \quad (21)$$

where $\hat{\eta}(t-1)$ is obtained by the observer.

Table 1. Parameters

Plant		Controller	
ω	2000 [rpm]	$k_{m_{iv}}$	0.3
θ_{OL}	60 [degCA]	k_τ	0.95
P_o	101.3 [kPa]	T_i	0.1 [s]
P_e	101.3 [kPa]	N_w	4
T_o	25 [degC]	N_p	6
T_e	400 [degC]	N_u	6
		Q	diag(10, 10)
		R	diag(1, 10)

Figure 4 shows the simulation results with Table 1. The filtered indicated torque $\tilde{\tau}_i$ follows the reference without offset. Notice that the intake pressure P_a follows the reference without offsets, but the IEGR ratio β_c has some steady state errors in the cases where the torque references are relatively small. That is because the model used in the controller is not completely equal to the plant.

Next, we demonstrate the controlled performace under various changes of parameters.

Case 1: Changes of P_o, T_o, T_e and P_e

Firstly, the outer pressure P_o in Table 1 is changed to 80 [kPa], which corresponds to the drive at high altitude around 2000 [m]. The simulation result is shown in Figure 5, where the behaviors of the filtered indicated torque $\tilde{\tau}_i$ and the IEGR ratio β_c are almost same as ones in the case of $P_o = 101.3$ [kPa]. But the intake valve lift u_{VL} becomes larger because the air is hard to flow into cylinders at high altitude.

Secondly, the outer temperature T_o in Table 1 is changed to -20 [degC], which corresponds to the drive in cold climates. Note that the controller does not know the actual outer temperature, so the controller uses 25 [degC] as the outer temperature. The simulation result is shown as dashed-dotted lines in Figure 6. The results on the filtered indicated torque $\tilde{\tau}_i$ and the IEGR ratio β_c are almost same as the case of $T_o = 25$ [degC]. Note that the

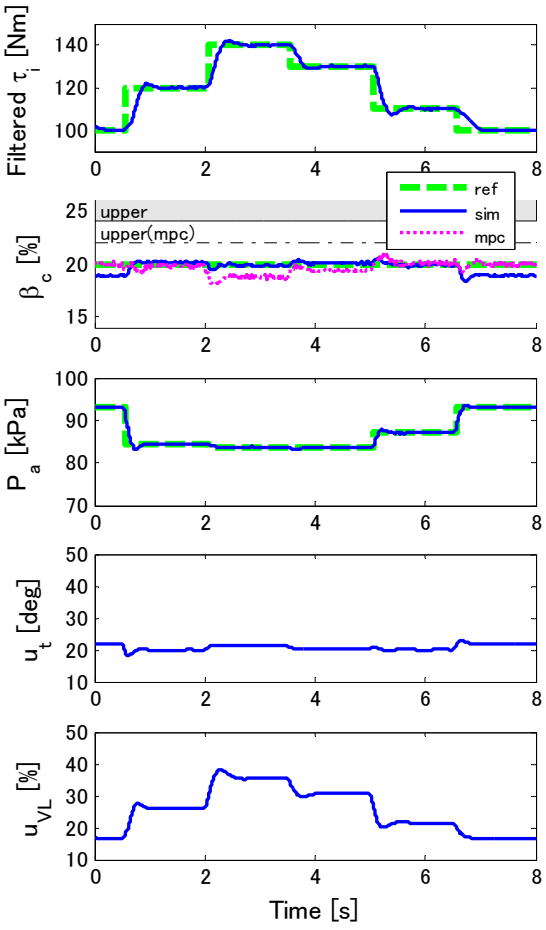

Fig. 4. Nominal controlled performance

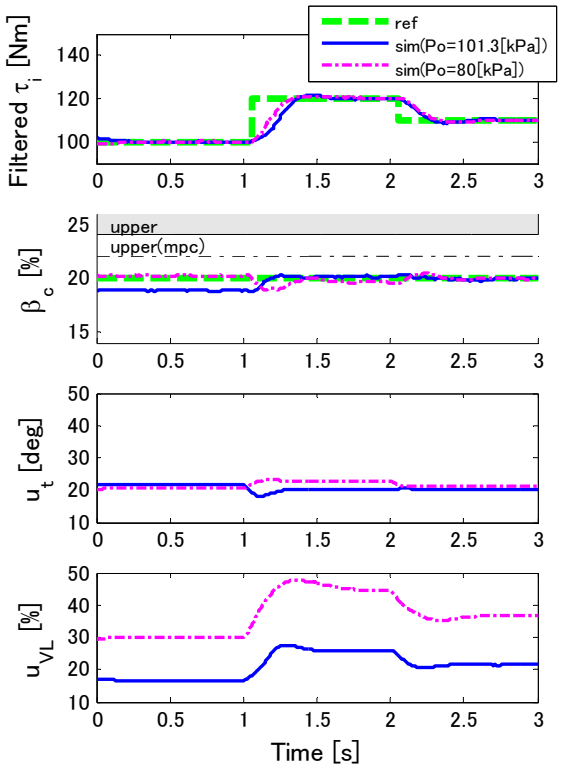

Fig. 5. Case 1: Change of P_o at High altitude

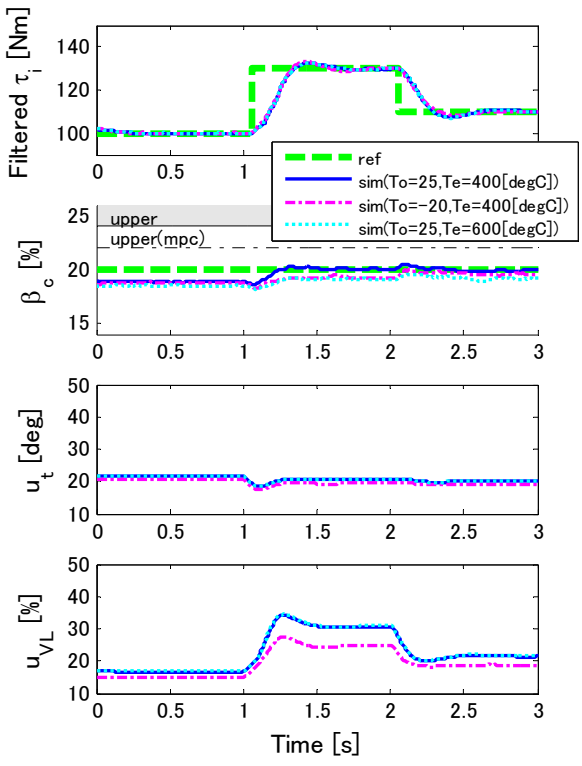

Fig. 6. Case 1: Change of T_o in cold climates and T_e due to estimation error

intake valve lift u_{VL} becomes smaller because the air is easy to flow into cylinders in cold climates.

Thirdly, the exhaust temperature T_e in Table 1 is changed to 600 [degC]. Note that the controller uses the estimated value of T_e as 400 [degC]. The simulation result is shown as dotted lines in Figure 6. The results on the filtered indicated torque $\tilde{\tau}_i$ and the IEGR ratio β_c, and the intake valve lift u_{VL} are almost equal to ones in the case of $T_e = 400$ [degC].

From the results shown in Figure 6, we can conclude that the proposed controller is robust against changes of T_o and T_e.

Finally, the exhaust pressure P_e in Table 1 is changed to 110 [kPa], but the controller is assumed to estimate P_e as 101.3 [kPa]. The simulation result is shown as dashed-dotted lines in Figure 7. Because the mass of backflow M_{ex} becomes larger in the case of $P_e = 110$ [kPa], the intake valve lift u_{VL} becomes larger so that the filtered indicated torque $\tilde{\tau}_i$ follows the reference. But, the IEGR ratio β_c becomes over the upper bound $\beta_c^{\max}$ although the predicted ratio $\beta_c(t+2)$ is under the virtual upper bound $\tilde{\beta}_c^{\max}$. That result concludes that the proposed controller is not robust against the mismatch between the actual exhaust pressure and the estimated exhaust pressure used in the controller.

Case 2: Deposit formation

The lubricating oil and the injected fuel may adhere to the throttle valve and the intake valves. This deposit formation could affect the flow of air through those valves, which can be regarded as changes of the effective opening areas of the throttle valve and the intake valve, A_t and A_{in}. In the simulation, it supposes that A_t decreases 10% after 1 [s] and also A_{in} decreases 10% after 2.5 [s]. As shown in Figure 8, the throttle angle u_t and the intake valve lift u_{VL} increase after 1 [s] and 2.5 [s], respectively. As a result, the controller realizes offset-free of the filtered indicated torque $\tilde{\tau}_i$.

Case 3: Variation of the valves' overlap

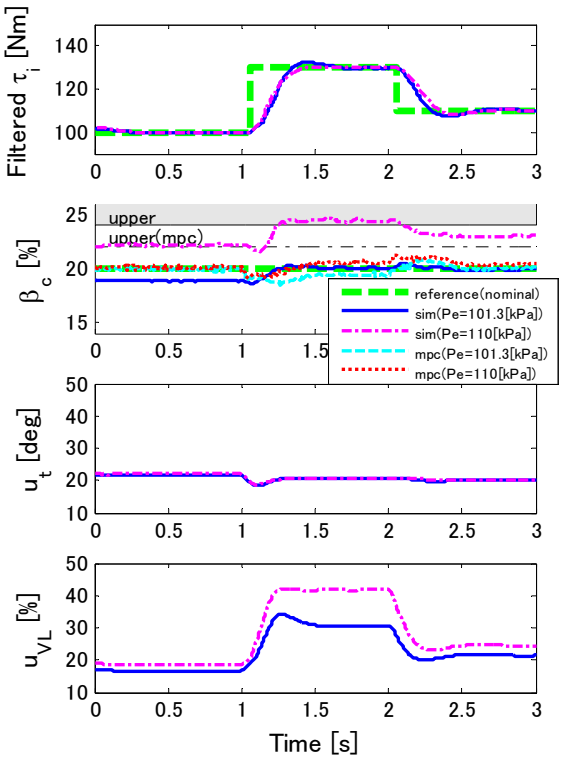

Fig. 7. Case 1: Change of P_e due to estimation error

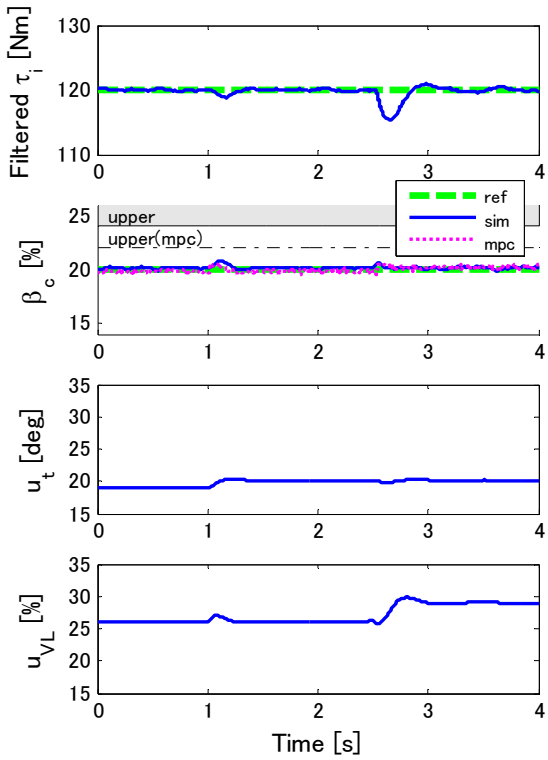

Fig. 8. Case 2: Deposit formation

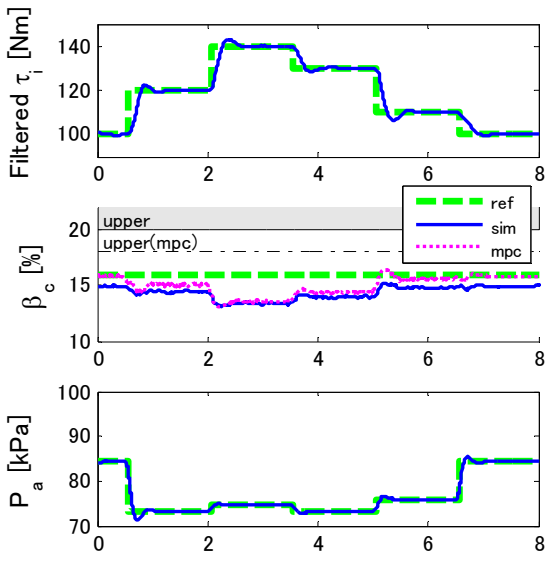

Fig. 9. Case 3: Variation of the valves' overlap

We consider the case where the overlap θ_{OL} is changed to 40 [degCA]. Notice that the IEGR reference $\beta_c^*(t)$ must be changed to 16 [%] from 20 [%] because in the case of $\theta_{OL} = 40$ [degCA], it is easy to see from the steady state analysis in Subsection 3.1 that $\beta_c^* = 20$ [%] is infeasible under the given torque reference. The simulation result is shown in Figure 9. The filtered indicated torque $\tilde{\tau}_i$ follows the reference without offset. The intake pressure P_a follows the reference without offsets, but the IEGR ratio β_c has some steady state errors. That is because the model used in the controller has relatively larger modeling error in the case of $\theta_{OL} = 40$ [degCA] than in the case of $\theta_{OL} = 60$ [degCA].

5. CONCLUSIONS

The present paper proposes the MPC for automotive engine torque considering IEGR. The features of the proposed method are as follows.

- The automotive engine has strong nonlinear properties with respect to the control inputs, i.e., the throttle angle and the intake valve lifts. The present paper proposed the control oriented automotive engine model, where the virtual control inputs, i.e., the mass flows through the throttle and the intake valves, are introduced to transform the original nonlinear model and constraints into the linear model and constraints.
- Based on the derived linear model and constraints, the MPC has been proposed, where the quadratic programming problem is solved every sampling period.
- Different types of inputs, the throttle angle and the intake valve lift, can be optimized considering the interaction, constraints such as the bounds of input levels, inputs speeds, and IEGR with the overlap.
- The proposed controller has a good controlled performance against deposit formation and at high altitude. Furthermore, the controller has the robustness in cold climates and against tolerance of opening areas and the estimation error of the exhaust temperatures. However, the controller does not have the robustness against the estimation error of the exhaust pressure because the exhaust pressure strongly influences the backflow through exhaust valves. Consequently, the actual IEGR ratio may be over the upper bound and the engine may misfire.

In the future, the following will be challenged:

- Precise estimation of the exhaust pressure
- Reduction of the computational cost
- Cooperation with the overlap control
- Control of both IEGR and EEGR (External Exhaust Gas Recirculation)

REFERENCES

Bemporad, A., Morari, M., Dua, V., and Pistikopoulos, E.N. (2002). The explicit linear quadratic regulator for constrained systems. *Automatica*, 38(1), 3–20.

del Re, L., Allgöwer, F., Glielmo, L., Guardiola, C., and Kolmanovsky, I. (2010). *Automotive Model Predictive Control*. Springer-Verlag, Berlin Heidelberg.

Gruenbacher, E., del Re, L., Kokal, H., M.Schmidt, and M.Paulweber (2008). Adaptive control of engine torque with input delays. In *Proc. of the 17th World Congress The International Federation of Automatic Control*, 9479–9484. Seoul, Korea.

Heywood, J. (1988). *Internal Combustion Engine Fundamentals*. McGraw-Hill, New York.

Huang, T., Liu, D., Javaherian, H., and Jin, N. (2008). Neural sliding-mode control of engine torque. In *Proc. of the 17th World Congress The International Federation of Automatic Control*, 9453–9458. Seoul, Korea.

Ingram, G.A., Franchek, M.A., and Balakrishnan, V. (2003). Spark ignition engine mass air flow control for precise torque management. *SAE Paper*, 2003–01–0624.

Jankovic, M., Frischmuth, F., Stefanopoulou, A., and Cook, J.A. (1998). Torque management of engines with variable cam timing. *IEEE Control Systems Magazine*, 18(5), 34–42.

Jimbo, T. and Hayakawa, Y. (2011a). A physical model for engine control design via role state variables. *Control Engineering Practice*, 19(3), 276–286.

Jimbo, T. and Hayakawa, Y. (2011b). Torque control for automotive engines with variable valves via air and burned gas flow-based design. *SICE Journal of Control, Measurement, and System Integration*. (to appear).

Langthaler, P. and del Re, L. (2008). Robust model predictive control of a diesel engine airpath. In *Proc. of the 17th World Congress The International Federation of Automatic Control*, 9485–9490. Seoul, Korea.

Leroy, T., Chauvin, J., Berr, F.L., Duparchy, A., and Alix, G. (2008). Modeling fresh air charge and residual gas fraction on a dual independent variable valve timings SI engine. *SAE Paper*, 2008–01–0983.

Liepmann, H. and Roshko, A. (1960). *Elements of Gasdynamics*. John Wiley and Sons, Inc., New York.

Maciejowski, J.M. (2002). *Predictive Control with Constraints*. Prentice Hall.

Maeder, U., Borrelli, F., and Morari, M. (2009). Linear offset-free model predictive control. *Automatica*, 45, 2214–2222.

Mayne, D.Q., Rawlings, J.B., Rao, C.V., and Scokaert, P.O.M. (2000). Constrained model predictive control: Stability and optimality. *Automatica*, 36, 789–814.

Muske, K.R., Jones, J.C.P., and Franceschi, E.M. (2008). Adaptive analytical model-based control for si engine air-fuel ratio. *IEEE Transactions on control systems technology*, 16(4), 763–768.

Ohata, A., Kako, J., Shen, T., and Ito, K. (2008). Introduction to the benchmark challenge on SICE engine start control problem. In *Proc. of the 17th World Congress The International Federation of Automatic Control*, 1048–1053. Seoul, Korea.

Taylor, C. (1985). *The Internal-Combustion Engine in Theory and Practice*. MIT Press, Cambridge, Mass, 2nd edition.